nature climate change

SUPPLEMENTARY INFORMATION

DOI: 10.1038/NCLIMATE2313

Recent trends in African fires driven by cropland expansion and El Niño to La Niña transition

Niels Andela* and Guido R. van der Werf

Earth and Climate cluster, Department of Earth Sciences, Faculty of Earth and Life Sciences, VU University, Amsterdam, the Netherlands

*e-mail: n.andela@vu.nl

1. Introduction

In this supplement we elucidate several aspects of our methods, results and the discussion. We provide additional details on the two explanatory variables used to drive the burned area model: the antecedent precipitation index (API, see section 2) and changes in cropland extent (dCROP, see section 3). We then detail the role of El Niño Southern Oscillation (ENSO) in driving burned area trends (section 4). After that, we discuss issues related to the relative short time series and the use of simple linear regression on trend estimation (section 5). Finally, the main findings are presented at country level to facilitate studies with a stronger regional focus and for local policy makers (section 6).

2. Precipitation induced burned area response

Antecedent precipitation has a strong impact on inter-annual variation of burned area[1,2]. Short averaging periods, including precipitation during or just before the fire season commences, were often associated with a negative precipitation – burned area response; while longer term precipitation averaging periods, including precipitation of preceding wet season(s), were often positively correlated with annual burned area (Fig. S1). The variability shown in Fig. S1 is largely in line with earlier work[1–3] with strong positive correlations mostly found in arid areas while strongest negative correlations were found in more humid areas. On top of these general patterns, considerable regional variation in averaging periods was observed. This regional variation could only partially be explained by mean annual precipitation and higher resolution studies may be able to clarify the drivers of these more localized patterns. Here we can only put forward several hypotheses for the regional variation in averaging periods:

1. When burned area in a given grid cell is mainly driven by biomass build up (dry regions), best correlation with the antecedent precipitation index is likely found when including about 8 months of precipitation prior to the burning season (including one

wet season) or about 20 months prior to burning season (including two wet seasons). Therefore, due to the strong seasonal precipitation cycle, large differences between neighbouring grid cells may be observed, where one grid cell might have slightly higher correlation for around 8 months and the other for around 20 months averaging periods. These periods correspond to the red and blue in Figure S1 which thus seem to indicate large spatial variability but which is in reality a very similar response.

2. We express moisture availability as a function of rainfall. In reality, drainage patterns, geomorphology, and other physical aspects of the landscape also govern moisture availability for plant growth which may therefore enhance regional variability in averaging periods and API – burned area response.
3. Landscape and vegetation aspects may also impact the averaging periods by affecting the fire regime (fire size, return period, duration, etc.). Regions with frequent large fires are for example more likely to have short averaging periods, because there is less 'carry over' effect of biomass build-up.
4. In a similar way, fire management also plays a role, affecting averaging periods by altering fire regimes.
5. For regions of infrequent fires or where weak correlation between API and the annual burned area anomaly was found, confidence in the averaging periods is limited. When longer time series become available, a better relation between precipitation and burned area can also be established for these regions.

Overall, we were able to explain the broad features but we do not fully resolve the spatial variability in averaging periods, which therefore remains a topic of future research.

In order to optimize the statistical model to predict inter-annual variation rather than the seasonal cycle, we based our model on precipitation and burned area anomalies instead of absolute values. In the model, API was calculated such that highest absolute Pearson's r was found between the API and annual burned area anomaly (see methods; Figs. S1a, S1c and S2). This way the model allowed for either positive or negative precipitation – burned area response for a given grid cell, where biomass build up was the main driver of positive responses and fuel moisture the main driver of negative responses (see methods). Only for a minor percentage (~3%) of the grid cells both a positive and a negative precipitation – burned area response was observed ($p<0.1$; Fig. S2). Therefore, we choose to represent both positive and negative response in one independent variable: API. This allowed us to keep the number of explanatory variables limited, important in light of the relatively short time series. At the

same time this simplification had only limited effect on the model outcome due to the small fraction of grid cells in which both effects played a significant role (Fig. S2). The implication is that API may have either a positive or a negative impact on annual burned area, depending on highest absolute Pearson's r for each grid cell. Several previous studies used similar approaches to model burned area – precipitation response[1,2] and to model vegetation – precipitation response[4–7].

3. Impact of cropland encroachment on burned area

The distribution of croplands was a key variable in explaining the distribution of burned area in northern Africa (Fig. 2a, for southern Africa a similar pattern was found). In addition, cropland extent showed some remarkable trends over the study period (Fig. 1c). We therefore included trends in cropland extent as an explanatory variable in the multiple linear regression model (see methods). One key result of our analyses is that the degree to which burned area was impacted by changes in cropland extent depended on both annual mean precipitation (MAP) and on the amount of natural vegetation already converted to cropland (Fig. 2b). The strongest negative impact was found in savannas of moderate annual precipitation (700-1200 mm yr^{-1}), where a decline of 1% in savannah area typically resulted in a decrease of annual burned area of about 0.4 to 0.5% (Fig. 2b). In the drier and more humid areas outside this precipitation range, the impact was generally smaller and sometimes even the opposite effect was observed, where increases in cropland area caused an increase in annual burned area. In more humid zones this may be due to human introduction of fires in ecosystems that naturally do not burn frequently. In drier regions we could not think of straightforward explanations, but these regions have a minor impact on our results because they fall outside the regions where most annual burned area occurs.

Based on the spatial distribution of annual burned area and croplands within savannah ecosystems (Fig. 2a), we expect that the impact of conversion of savannas into cropland found by our model was conservative. Mean annual burned area in untouched savannas was found to be around 44% (indicating that on average, 44% of a grid cell burned in a given year) in northern Africa, while savannas with between 1 and 20% cropland extent had about half the annual burned area on average. This suggests a much stronger response of burned area to cropland conversion (in this case about 2% per percent cropland increase) than found by our model (maximum of about 0.5%), especially at the onset of land cover conversion (Fig. 2). Besides this quantitative result based on the spatial distribution of annual burned area there

are several other reasons to believe that our model might indeed be on the conservative side. Due to the short time series we have used large MAP – cropland extent bins to determine the effect of cropland conversion on annual burned area. This resulted in a robust model, assuring that modelled trends correspond to actual physical processes, but reduced the explanatory power of the model. Moreover there may be a time delay which was better captured by the spatial analysis. Finally, the averaging period *T* was chosen such that highest absolute correlation between the running mean of the monthly precipitation anomaly and the annual burned area anomaly was found. API was thus selected based on highest absolute correlation with the total burned area signal, including the cropland driven trend. Because inter-annual variation in burned area was much larger than the underlying trend caused by cropland expansion this effect was small, but expected to favour API as a driver of observed trends over dCROP. This may have somewhat reduced the trends driven by cropland extension as explained by our model. The advantage of deriving API based on strongest correlation was that it will represent actual physical processes. Alternatively API could be selected by optimizing the model (eq. 1), but such an approach would easily lead to over fitting, neglecting the physical processes underlying the model.

4. The impact of ENSO on annual burned area

For several African regions ENSO is known to be related to precipitation variation[8] and vegetation dynamics[9]. It was therefore not surprising to see a clear relation between variations in ENSO and annual burned area in Africa (Fig. 3). The effect is not straightforward because of the dualistic character of precipitation – burned area patterns where increases in precipitation short before or during the burning season will have a negative effect on annual burned area, while longer term increases in precipitation may increase annual burned area through the process of biomass build up (see also section 2). In addition, the ENSO – rainfall correlation is not uniform but shows substantial regional variability. Overall, we found that ENSO was mostly negatively related to burned area in southern Africa and positively in northern Africa (Figs. 3 and S3). Because part of the declining trend in annual burned area in northern Africa could be explained by cropland encroachment, the observed trend in annual burned area was more negative than would be expected from the decrease in the Multivariate ENSO Index (MEI) alone (Fig. S3).

5. Trend analysis

In drier regions of southern Africa, net primary production is the main limitation to annual burned area and inter-annual variation in precipitation and burned area is large. Due to this high inter-annual variability and the short time series (12 yrs) trends may become somewhat sensitive to outliers, for example if in a given year rainfall rates were high enough to support a continuous fuel bed that boosted burned area substantially compared to other years when this was not the case. We compared the results of simple linear regression to trends as calculated by the non parametric Theil-Sen estimator of slope, which is insensitive to outliers[10,11]. Results were very similar for most of Africa, but considerable differences were found for Botswana and Namibia, where some of the trends seem to be caused by strong inter-annual variation. However, when using Theil-Sens estimator of slope some trends disappeared in the observations but remained in the model, causing unrealistic discrepancies between the model and observations. Therefore, we decided to calculate trends using simple linear regression.

6. Country-level results

Country-level results allow for increased regional insights in the effects of policy and socio-economic developments on annual burned area and are therefore essential for regional studies and policymaking. The fractional change in annual burned area for each country was calculated as the ratio of the observed absolute trend and the mean burned area over the study period (Table S1). Due to the effects of ENSO on regional precipitation, all countries that faced a large net increase in annual burned area over the study period are located in southern Africa, while countries with a large net decrease are located in northern Africa. This corresponds to the MEI being positively correlated to annual burned area for most of northern Africa and negatively correlated for most of southern Africa (Fig. 3). For most countries of southern Africa no large scale changes in burned area due to savannah – cropland conversion were observed during the study period (Fig. 1e). A notable exception is Zimbabwe, where according to our model an increase in annual burned area could be explained by increased precipitation but also due to declined agricultural activity, possibly caused by the fast land reforms of the past decade[12]. In northern Africa, a mix of precipitation and changes in cropland area were driving the observed decline in annual burned area. Observed trends in Cameroon, Ghana and Central Africa were largely explained by changes in precipitation, while burned area trends in Nigeria, Ivory Coast and Mali could be explained by a combination of changes in cropland area and precipitation. In Burkina Faso and Benin,

cropland expansion caused most of the decline in annual burned area with precipitation playing a smaller role.

References

1. Archibald, S., Nickless, A., Govender, N., Scholes, R. J. & Lehsten, V. Climate and the inter-annual variability of fire in southern Africa: a meta-analysis using long-term field data and satellite-derived burnt area data. *Glob. Ecol. Biogeogr.* **19,** 794–809 (2010).

2. Archibald, S., Nickless, A., Scholes, R. J. & Schulze, R. Methods to determine the impact of rainfall on fuels and burned area in southern African savannas. *Int. J. Wildl. Fire* **19,** 774–782 (2010).

3. Van der Werf, G. R., Randerson, J. T., Giglio, L., Gobron, N. & Dolman, A. J. Climate controls on the variability of fires in the tropics and subtropics. *Global Biogeochem. Cycles* **22,** GB3028 (2008).

4. Wessels, K. J. *et al.* Can human-induced land degradation be distinguished from the effects of rainfall variability? A case study in South Africa. *J. Arid Environ.* **68,** 271–297 (2007).

5. Evans, J. & Geerken, R. Discrimination between climate and human-induced dryland degradation. *J. Arid Environ.* **57,** 535–554 (2004).

6. Herrmann, S. M., Anyamba, A. & Tucker, C. J. Recent trends in vegetation dynamics in the African Sahel and their relationship to climate. *Glob. Environ. Chang.* **15,** 394–404 (2005).

7. Andela, N., Liu, Y. Y., van Dijk, A. I. J. M., de Jeu, R. A. M. & McVicar, T. R. Global changes in dryland vegetation dynamics (1988–2008) assessed by satellite remote sensing: comparing a new passive microwave vegetation density record with reflective greenness data. *Biogeosciences* **10,** 6657–6676 (2013).

8. Dai, A. & Wigley, T. M. L. Global patterns of ENSO-induced precipitation. *Geophys. Res. Lett.* **27,** 1283–1286 (2000).

9. Anyamba, A., Tucker, C. & Mahoney, R. From El Niño to La Nina: vegetation response patterns over east and southern Africa during the 1997-2000 period. *J. Clim.* **15,** 3096–3103 (2002).

10. Sen, P. Estimates of the regression coefficient based on Kendall's tau. *J. Am. Stat. Assoc.* **63,** 1379–1389 (1968).

11. Theil, H. A rank-invariant method of linear and polynomial regression analysis. I. *Nederl. Akad. Wetensch., Proc.* **53,** 386–392 (1950).

12. Scoones, I. *et al.* Zimbabwe's land reform: challenging the myths. *J. Peasant Stud.* **38,** 967–993 (2011).

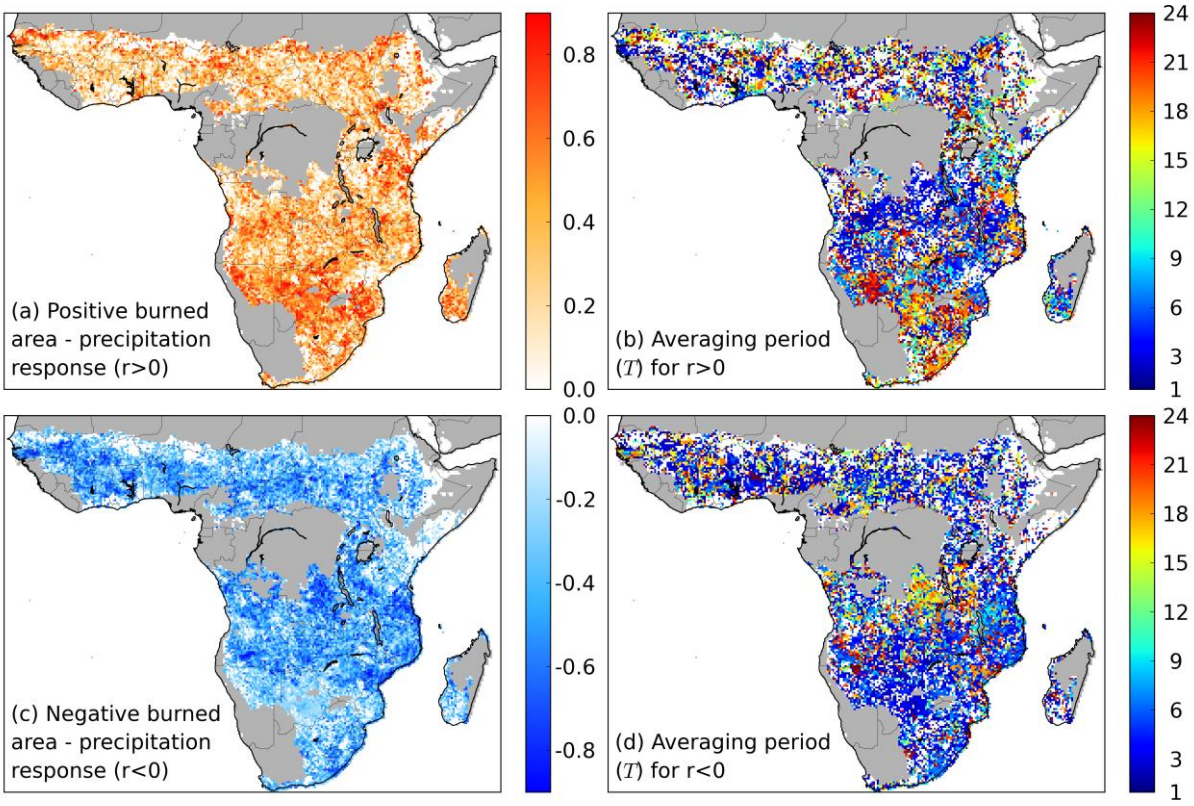

Figure S1. Optimal correlation (Pearson's r) between API and the annual burned area anomaly and corresponding averaging periods (*T*) in months. **a**, Strongest positive correlation between API and annual burned area and **b**, corresponding averaging periods. **c**, Strongest negative correlation between API and annual burned area and **d**, corresponding averaging periods. Areas with precipitation rates smaller than 400 or larger than 1500 mm yr^{-1} are masked grey while oceans and areas of no correlations are shown in white.

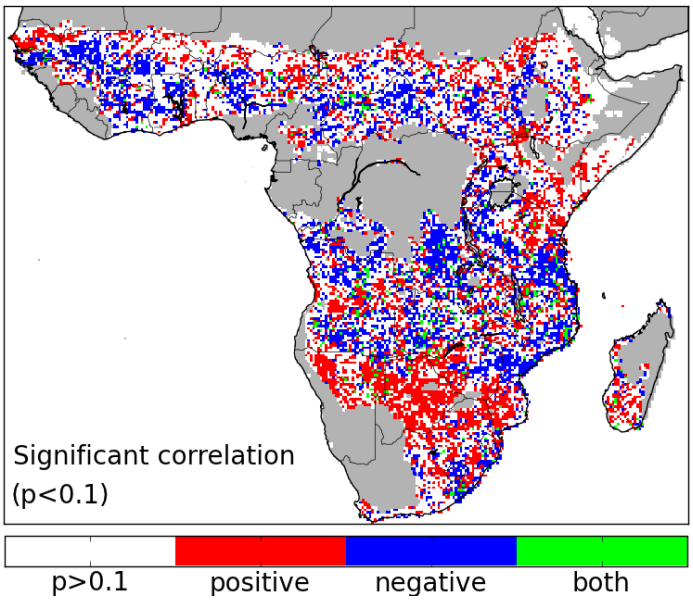

Figure S2. Areas where a significant (p<0.1) positive, negative or both effect(s) between API and the annual burned area anomaly are found. Areas with precipitation rates smaller than 400 or larger than 1500 mm yr^{-1} are masked in grey.

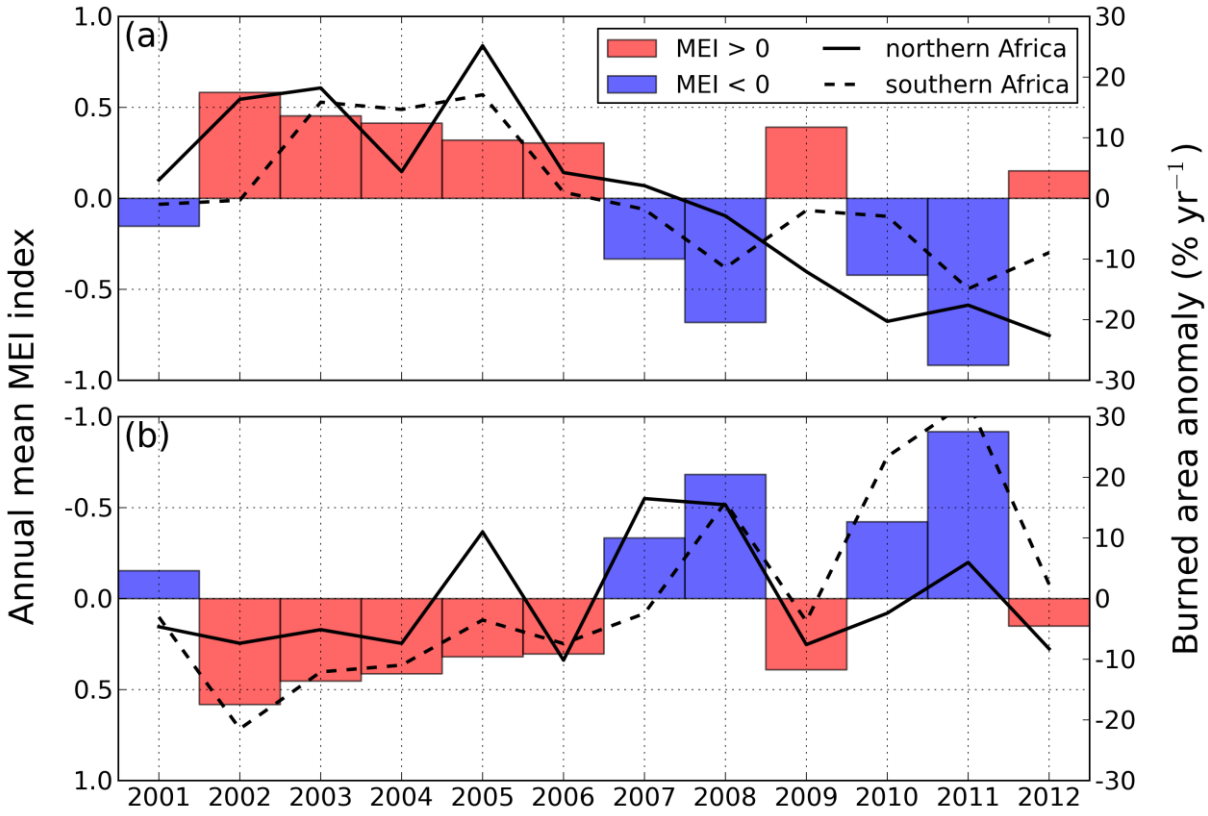

Figure S3. Annual mean MEI values and burned area anomalies for northern and southern Africa, separated by their response to the MEI (see Fig. 3). **a**, Areas with positive correlation (Pearson's r) between the burned area anomalies and the MEI (each percent change in burned area corresponds to 0.94Mha and 0.64Mha for northern and southern Africa, respectively). **b**, Areas with negative correlation between the burned area anomalies and the MEI (1% corresponds to 0.41Mha and 0.84Mha for northern and southern Africa, respectively). Note the inversed y-axis corresponding to the annual mean MEI. Areas with precipitation rates smaller than 400 or larger than 1500 mm yr^{-1} are not included.

Table S1. Annual burned area, observed trend, trends explained by precipitation and trends explained by cropland encroachment. Countries with trends smaller than 1000 km^2 yr^{-2} are not shown.

Country	Burned area (1000 km^2 yr^{-1})	Observed trend (% 10 yr^{-2})	Driver: precipitation (% 10 yr^{-2})	Driver: cropland encroachment (% 10 yr^{-2})
Nigeria	80.4	-61.4	-14.6	-20.4
Burkina Faso	30.3	-53.4	-10.4	-19.8
Cameroon	30.6	-51.0	-23.5	-3.3
Ivory Coast	30.0	-49.9	-12.5	-8.7
Benin	25.4	-48.1	-3.4	-8.6
Mali	77.1	-27.8	-8.8	-7.3
Chad	109.3	-27.8	-7.7	-3.7
Ghana	67.7	-24.0	-5.2	-0.9
Central Africa	213.8	-18.7	-5.4	0.0
Sudan	407.7	-7.5	-1.7	-1.4
Mozambique	191.8	12.8	4.7	0.9
Zimbabwe	36.0	60.3	16.3	5.1
Botswana	62.4	76.4	42.8	-0.2
Namibia	47.9	99.5	56.2	0.2
Northern Africa	1260.0	-21.4	-5.2	-4.3
Southern Africa	1369.7	8.8	4.5	0.3